

## Electrons confined on the surface of a sphere in a magnetic field

Ju H. Kim and I. D. Vagner

*Department of Physics and Astronomy, The Johns Hopkins University, 34th and North Charles Street, Baltimore, Maryland 21218  
and Max-Planck-Institute für Festkörperforschung, Hochfeld-Magnet-Labor, Boîte Postale 166X,  
F-38042 Grenoble CEDEX, France*

B. Sundaram

*Department of Physics and Astronomy, The Johns Hopkins University, 34th and North Charles Street, Baltimore, Maryland 21218  
(Received 26 June 1992)*

We derive an analytic expression for the quantum-mechanical spectrum of noninteracting electrons restricted to move on the surface of a sphere in a uniform external magnetic field. The field dependence of the energy levels leads to a complex level crossing structure which is manifested in the magnetic properties. For a fixed number of electrons, the magnetization exhibits irregular discontinuities at low fields while aperiodic oscillations occur at higher field values. The magnetic susceptibility exhibits sharp spikes and "jumps," as the chemical potential crosses the energy gaps between adjacent energy levels.

Simple model systems have often served as useful paradigms to gain insight into the behavior of real systems. A notable example is the energy spectrum of a free electron in a magnetic field<sup>1</sup> (Landau levels), which provides the basis for understanding a wide range of physical phenomena, such as oscillations in thermodynamic and transport properties in metals and semiconductors. In a two-dimensional electron-gas system, as a consequence of the Landau quantization, the magnetization<sup>2</sup> and the magnetic susceptibility<sup>3</sup>  $\chi$  exhibit exponentially sharp (proportional to inverse temperature) "jumps" and spikes, respectively, at low temperatures. These aspects of electron gases in confined geometries have been the subject of many investigations. For example, Azbel,<sup>4</sup> and Sivan and Imry<sup>5</sup> showed that edge states reduce the sharpness of diamagnetic susceptibility spikes. Nakamura and Thomas showed,<sup>6</sup> in a temperature-independent context, that susceptibility spikes arise from a complex network of avoided level crossings. The diamagnetic spikes have been experimentally observed in inversion layers<sup>7</sup> by Fang and Stiles, and in a Br<sub>2</sub>-GIC (graphite intercalated compound) system<sup>8</sup> by Markiewicz and co-workers. Calculations on a small metallic cluster<sup>9</sup> also suggest the existence of sharp features that resemble the susceptibility spikes.

More recently, the magnetotransport properties in mesoscopic systems such as electrons confined to a ring, and by potentials exhibiting parabolic or spherical symmetry, have attracted considerable attention due to advances in fabrication technology. For example, edge states<sup>10</sup> and persistent currents in a mesoscopic metallic ring<sup>11,12</sup> have been a focus of both theoretical and experimental<sup>13</sup> investigations. However, the problem of electrons confined in a spherically symmetric potential in a homogeneous magnetic field remains unsolved. An example of this is the "diamagnetic Kepler problem,"<sup>14</sup> which proved useful in the study of excitons in semiconductors.<sup>15</sup>

We consider the effect of a uniform magnetic field on the quantum-mechanical spectrum of noninteracting electrons whose motion is constrained to the surface of a sphere. In the absence of the field, the problem is fully degenerate and, as expected, the field breaks this degeneracy. However, the confined motion is analogous to having a nonuniform field in the case of a restricted planar geometry. We demonstrate that this leads to interesting level crossing effects in the spectrum that are reflected in the magnetic response of the system.

Consider the case of a single electron confined to the surface of a sphere by a potential  $V_0$  as described by the Hamiltonian

$$H = \frac{1}{2m} \left[ \mathbf{p} - \frac{e}{c} \mathbf{A} \right]^2 - V_0 \delta(r - R), \quad (1)$$

where, for simplicity, we ignore spin-dependent terms.  $R$  is the radius of the sphere and we choose the symmetric gauge  $\mathbf{A} = B(-y, x, 0)/2$  such that the externally applied magnetic field  $B$  points in the  $z$  direction. Since the radial motion is absent in the limit  $V_0 = \infty$ , it is convenient to express Eq. (1) in spherical polar coordinates as

$$H = -\frac{\hbar^2}{2mR^2} \left[ \frac{1}{\sin\theta} \frac{\partial}{\partial\theta} \left[ \sin\theta \frac{\partial}{\partial\theta} \right] - \frac{L_z^2}{\sin^2\theta} + \frac{mR^2\omega_c}{\hbar^2} L_z + \left[ \frac{mR^2\omega_c}{2\hbar} \right]^2 \sin^2\theta \right], \quad (2)$$

where  $\omega_c = eB/mc$  is the cyclotron frequency and  $L_z = -i\hbar\partial/\partial\phi$  is the  $z$  component of the angular momentum operator. In the magnetic field, the total angular momentum is not conserved, but  $L_z$  is still a conserved quantity. This allows for separability in the variables  $\theta$  and  $\phi$ . Considering  $\Psi = \Psi_\theta\Psi_\phi$  and using  $L_z\Psi = l_z\hbar\Psi$  in the Schrödinger equation results in a wave equation for  $\Psi_\theta$ . This is further simplified by changing to  $x = \cos\theta$

and considering  $\Psi_\theta = (1-x^2)^{n/2}P(x)$ . For  $n = |l_z|$ , Eq. (2) may be reduced to a special case of the generalized spheroidal wave equation<sup>16</sup>

$$(1-x^2)\frac{d^2P}{dx^2} - 2(n+1)x\frac{dP}{dx} + \left[ \lambda^2 x^2 + \frac{2mR^2 E}{\hbar^2} - n(n+1) \right] P = 0. \quad (3)$$

Here,

$$\lambda = mR^2 \omega_c / 2\hbar = \Phi / \Phi_0,$$

$$n(n+1) - \tilde{E} = \frac{1 \times 2 \lambda^2 f_n(1,3)}{1 - \tilde{E} f_n(1,3) - \frac{3 \times 4 \lambda^2 f_n(1,5)}{1 - \tilde{E} f_n(3,5) - \frac{5 \times 6 \lambda^2 f_n(3,7)}{1 - \tilde{E} f_n(5,7) - \dots}}, \quad (4)$$

where  $f_n(i,j) = (n+i)!/(n+j)!$ . Similarly, an odd power series  $P(x) = \sum_{m=0}^{\infty} b_{2m+1} x^{2m+1}$  results in

$$(n+2)(n+1) - \tilde{E} = \frac{2 \times 3 \lambda^2 f_n(2,4)}{1 - \tilde{E} f_n(2,4) - \frac{4 \times 5 \lambda^2 f_n(2,6)}{1 - \tilde{E} f_n(4,6) - \frac{6 \times 7 \lambda^2 f_n(4,8)}{1 - \tilde{E} f_n(6,8) - \dots}}. \quad (5)$$

Each of the continued fractions admits an infinite number of roots that correspond to bound states of an electron in an infinite confining potential. By contrast, in a real system the number of bound states is limited by the finite value of  $V_0$  (work function) as well as by the field strength. In the zero-field limit, the roots are given by  $\tilde{E} = l(l+1)$ , where the (orbital angular momentum) quantum number  $l$  labels the quantized energy levels. Each  $l$  level is  $(2l+1)$ -fold degenerate. The degeneracy in  $l_z$  is lifted in the magnetic field, and the field dependence of the energy level is given by

$$E_{(l,l_z)}(\lambda) = \frac{\hbar^2}{2mR^2} [\tilde{E}_{(l,l_z)}(\lambda) + \lambda^2 + 2l_z \lambda], \quad (6)$$

where  $\tilde{E}$  are the roots of Eqs. (4) and (5). For the remainder of the paper, we denote each state by  $(l, l_z)$ . Note that in low fields, the energy of a  $-l_z$  state is lower than its zero-field value.

In Fig. 1 we show the variation of  $E_{(l,l_z)}$  with magnetic flux  $\Phi/\Phi_0$ , for  $l < 9$ , where the continued fractions were solved numerically. The complicated field dependence of the energy spectrum is clearly illustrated. The solid and dotted lines represent energy levels for the even and odd values of  $l$ , respectively. There are several features of the spectrum that are worth noting. Although the states  $(l, l_z)$  and  $(l+1, l_z)$  are nondegenerate in low fields, they become degenerate at higher field values. Furthermore, the field strength at which this occurs increases with  $(l, l_z)$ . The complex level crossing behavior shown in the figure arises from the field dependence of  $(l, -l_z)$  states.

where  $\Phi$  is the flux through the equatorial plane and  $\Phi_0$  is a flux quantum. To illustrate, for  $R = 100 \text{ \AA}$ ,  $\lambda = 1$  corresponds to the field strength of 13 T.

Although  $P(x)$  may be expressed in terms of the associated Legendre polynomials, it is difficult to calculate the spectrum directly from this approach. We therefore consider a Frobenius method by expressing  $P(x)$  as either an even or odd power series corresponding, respectively, to symmetric and antisymmetric solutions. Substituting an even power series expansion  $P(x) = \sum_{m=0}^{\infty} a_{2m} x^{2m}$  into Eq. (3) leads to a recursion relation for the coefficient  $a_{2m}$ . The indicial equation leads to the spectrum being given by the solutions of the following continued fraction:

The relative importance of the linear versus the quadratic dependence on the magnetic field leads to a decrease at low fields while an increase results at high fields. The critical field where the trend reverses increases with  $l_z$ .

As a result of the level crossings, it is clear that on considering  $N$  noninteracting electrons, the quantum number

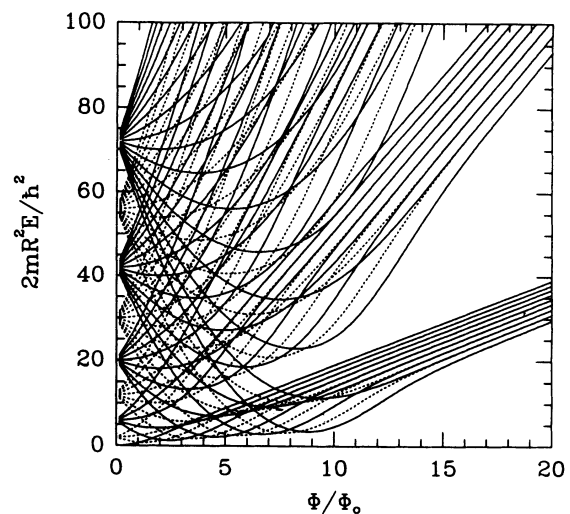


FIG. 1. The energy spectrum as a function of a magnetic field for states with  $l < 9$ . The solid and dotted lines represent even and odd values of  $l$ , respectively. In high fields, the formation of manifolds of states resembling Landau levels is also illustrated.

$(l, l_z)$  for the highest occupied state is changed with  $\Phi/\Phi_0$ . For small values of  $N$ , the level crossing structure is simple but it becomes more complicated as  $N$  increases. For example, when  $N=2$  the level crossing pattern with the increase in the field is given by the sequence

$$(0,0) \rightarrow (1,-1) \rightarrow (2,-2) \rightarrow (3,-3) \rightarrow \dots,$$

where each level crossing changes the quantum numbers by  $l \rightarrow (l+1)$  and by  $l_z \rightarrow (l_z-1)$ . For  $N=10$ , the low-field sequence is given by

$$(2,-2) \rightarrow (1,-1) \rightarrow (2,-1) \rightarrow (3,-3) \rightarrow \dots,$$

while the high-field structure is

$$\dots \rightarrow (5,-5) \rightarrow (1,-1) \rightarrow (6,-6) \rightarrow (2,-2) \rightarrow \dots.$$

At low fields, a simple pattern for the changes in  $(l, l_z)$  due to level crossings is absent but it appears as the field is increased. This appearance is the direct consequence of states forming manifolds that resemble Landau levels. Although the number of states in a given manifold increases with the field, the degeneracy does not. As shown in Fig. 1, with increasing field strength  $(l, -l)$  and  $(l, -l+1)$  states form the lowest manifold while the next-lowest manifold consists of  $(l, -l+2)$  and  $(l, -l+3)$  states.

This level crossing behavior leads to complicated structures in the field dependence of the magnetization and the magnetic susceptibility. We calculate these properties from the free energy  $F = \Omega - \mu$  for fixed  $N$ . Here, the thermodynamic potential

$$\Omega = (1/\beta) \sum_{l, l_z} \ln \{ 1 + \exp[-\beta(E - \mu)] \},$$

where  $\mu$  denotes the chemical potential and  $\beta = 1/kT$ . We express the magnetization per unit area as

$$M = \frac{1}{2\Phi_0} \sum_{l_z, l} f(E) \frac{\partial E}{\partial \lambda}, \quad (7)$$

where  $f(E)$  is the Fermi function. From Eq. (7), we obtain the magnetic susceptibility

$$\chi = \frac{\pi R^2}{2\Phi_0} \sum_{l, l_z} \left[ f(E) \frac{\partial^2 E}{\partial \lambda^2} - \frac{\beta g_E}{4} \frac{\partial E}{\partial \lambda} \left[ \frac{\partial \mu}{\partial \lambda} + \frac{\partial E}{\partial \lambda} \right] \right], \quad (8)$$

where  $g_E = \cosh^{-2}[\beta(E - \mu)/2]$ , and the derivative of the chemical potential with respect to the field is obtained from the normalization condition  $N = \sum_{l, l_z} f(E)$ ,

$$\left[ \frac{\partial \mu}{\partial \lambda} \right] = \frac{\sum_{l, l_z} g_E (\partial E / \partial \lambda)}{\sum_{l, l_z} g_E}. \quad (9)$$

For fixed  $N$ , the chemical potential oscillates with the field. These oscillatory features in  $\mu$  as a function of  $\Phi/\Phi_0$  arise from level crossings that decrease the free energy. As we show below, this variation is crucial for the existence of discontinuities in the magnetization and spikes in the magnetic susceptibility. It is worth noting here that the last two terms in Eq. (8) are not considered

in the temperature-independent formalism of Ref. 6. There, the curvature of the energy levels is solely responsible for the spikes in  $\chi$ , and this allows for the correlation of nonmonotonic variations in  $\chi$  with nonintegrability in the classical treatment of the problem.<sup>6</sup>

We plot the magnetization as a function of  $\Phi/\Phi_0$  in Fig. 2 for  $N=2, 10$ , and 30 electrons on the sphere. In all cases, we consider the temperature  $\beta=500$ , in units of  $\hbar^2/2mR^2$ . The magnetization exhibits irregular sawtooth oscillations with the field. The discontinuous jumps correspond to level crossings that lower the free energy. Furthermore, these oscillations become more pronounced as well as more irregular as  $N$  (Fermi energy) is increased. In contrast, with increasing field value, the magnetization exhibits regular sawtooth oscillations. This is most clear for the case of  $N=2$  and occurs due to the highest occupied state changing  $(l, l_z)$  with a regular pattern at a level crossing, as shown earlier. These oscillations are similar to the de Hass-van Alphen effect for electron gases. It is the absence of such a pattern (in low fields) that gives rise to the irregular oscillations seen in the curves for  $N=10$  and 30. However, the magnetization oscillations become regular as the field is increased although they are aperiodic in the normalized flux  $\Phi/\Phi_0$ . The transition from the irregular to regular oscillations depends on  $N$ . For few electrons, this transition occurs in low fields, but a stronger field is necessary as the number of electrons increase.

In Fig. 3, we plot the magnetic susceptibility as a function of  $\Phi/\Phi_0$  for  $N=2, 10$ , and 30. In understanding the variations in  $\chi$ , it is worth noting that both diamagnetic and paramagnetic contributions have been considered. The discontinuities in the magnetization curve in Fig. 3 appear as spikes (diamagnetic) in the magnetic susceptibility. These spikes are followed by a paramagnetic susceptibility jump because two levels that cross do not have

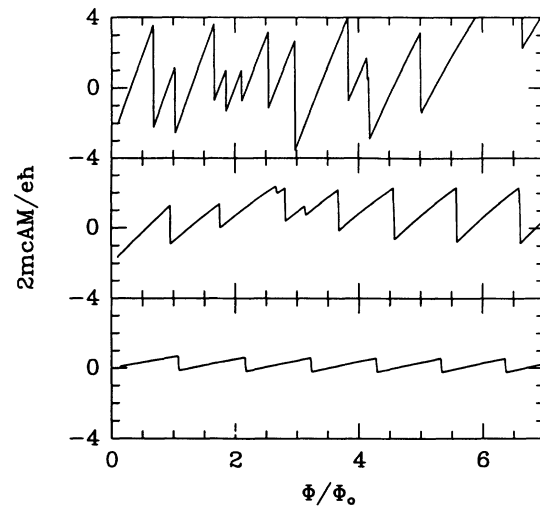


FIG. 2. Curves showing magnetization as a function of  $\lambda$  for electron occupation number  $N=2$  (bottom), 10 (middle), and 30 (top panel). The temperature  $\beta=500$  in units of  $\hbar^2/2mR^2$ . Discontinuities in the magnetization correspond to decreases in the free energy due to the level crossing structure in Fig. 1.

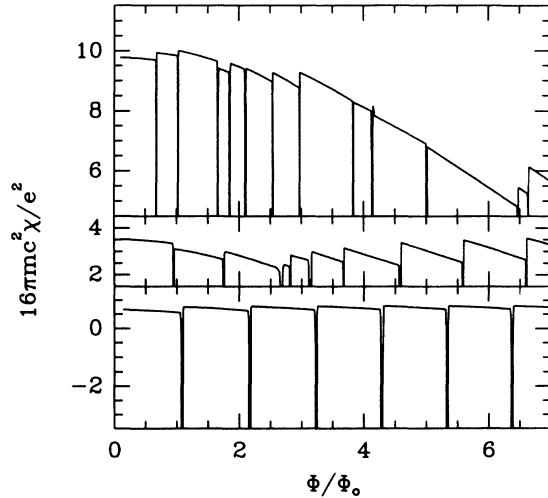


FIG. 3. Magnetic susceptibility as a function of  $\lambda$  for  $N=2$  (bottom), 10 (middle), and 30 (top panel). The width of the spikes arise from the temperature dependence of the magnetization discontinuities.

the same field dependence. Furthermore, the width and the amplitude of the spikes are not identical, since each discontinuity has a slightly different temperature dependence. A small jump in the magnetization curve leads to strong temperature dependence in the magnetic susceptibility. In low fields, the paramagnetic contribution depends on the field as well as the number of electrons  $N$ . The field dependence of  $\chi$  is most pronounced for  $N=30$  where the susceptibility gradually decreases as the field is increased. This trend reflects that as the highest occupied state is in the lowest manifold (at high fields), there is an approximate linear dependence of the spectrum on the field. Furthermore, the paramagnetic contribution to  $\chi$  increases with the number of electrons (from bottom to top panel). When  $N$  exceeds some critical value  $N_c$ ,  $\chi$  may become larger than the value  $1/4\pi$ . In this situation, the system becomes thermodynamically unstable with respect to the magnetic phase separation.<sup>2,12</sup>

In summary, we have solved the quantum-mechanical problem of noninteracting electrons confined on a sphere

in a magnetic field. We recognize simple patterns in  $(l, l_z)$  that account for the complex level crossing structure in the energy spectrum, which arises from the field dependence of  $(l, l_z)$  states. These patterns are manifested in physical effects such as the magnetization oscillations and discontinuities and spikes in the magnetic susceptibility. We observe that, at higher field values, the magnetization for electrons in the ground state exhibits regular oscillations with the flux  $\Phi$  through the equatorial plane. There is no clear period, although an approximate one would be close to the flux quantum  $\Phi_0$ . The first several oscillations indicate variable periodicity, always larger than  $\Phi_0$ , which decreases with the field. This is consistent with the Aharonov-Bohm effect in the spherical geometry where the wave function is centered away from the equatorial plane. With increasing number of electrons, the low-field magnetization oscillations are irregular, while the regular oscillations discussed above appear as the field is increased. The complicated low-field energy spectra condense into well-defined manifolds in the high-field limit. These manifolds resemble the Landau fan of energy levels and, for example, the lowest manifold consists of  $(l, -l)$  and  $(l, -l+1)$  states. In general, the  $n$ th manifold consists of all states with labels  $(l, -l+2n)$  and  $(l, -l+2n+1)$  and the number of states in each manifold increases with the magnetic field.

In conclusion, we suggest a model for mesoscopic systems where the interesting thermodynamic properties arise from the interplay between the confined geometry and applied magnetic field. This model may be realized in a small hollow spherical conductor where our solutions can be modified to account for finite, uniform thickness or in members of the fullerenes.<sup>17</sup> More realistic analysis may require inclusion of electronic interactions that would lead to nonintegrable dynamics,<sup>6</sup> as would nonsystematic deformations, such as variable thickness, of the confining geometry.

We acknowledge helpful discussions with D. Reich and Z. Tešanović. This research was supported by a grant from the German-Israeli Foundation for Science Research and Development, Grant No. G-112-279.7/88. J. H. K. was supported in part by the David and Lucile Packard Foundation.

<sup>1</sup>L. D. Landau, *Z. Phys.* **64**, 629 (1930).

<sup>2</sup>R. Peirls, *Z. Phys.* **81**, 186 (1933); I. D. Vagner *et al.*, *Phys. Rev. Lett.* **51**, 1700 (1983); J. J. Quinn, *Nature* **317**, 389 (1985).

<sup>3</sup>I. D. Vagner and T. Maniv, *Phys. Rev. B* **32**, 8398 (1985).

<sup>4</sup>M. Ya. Azbel', *Solid State Commun.* **54**, 127 (1985).

<sup>5</sup>U. Sivan and Y. Imry, *Phys. Rev. Lett.* **61**, 1001 (1988).

<sup>6</sup>K. Nakamura and H. Thomas, *Phys. Rev. Lett.* **61**, 247 (1988).

<sup>7</sup>F. F. Fang and P. J. Stiles, *Phys. Rev. B* **28**, 6992 (1983).

<sup>8</sup>B. Maheswaran *et al.*, *Phys. Rev. B* **39**, 1946 (1989).

<sup>9</sup>J. M. van Ruitenbeek *et al.*, *Phys. Rev. Lett.* **67**, 640 (1991); for a review, see J. A. A. J. Perenboom *et al.*, *Phys. Rep.* **78**, 73 (1981).

<sup>10</sup>B. Halperin, *Phys. Rev. B* **25**, 2185 (1982).

<sup>11</sup>M. Buttiker *et al.*, *Phys. Lett.* **96A**, 365 (1983); R. Landauer and M. Buttiker, *Phys. Rev. Lett.* **54**, 2043 (1985).

<sup>12</sup>D. Wohlleben *et al.*, *Phys. Rev. Lett.* **66**, 3191 (1991).

<sup>13</sup>L. P. Lévy *et al.*, *Phys. Rev. Lett.* **64**, 2074 (1990).

<sup>14</sup>M. Gutzwiller, *Chaos in Classical and Quantum Mechanics* (Springer-Verlag, New York, 1990).

<sup>15</sup>H. Hasegawa, *Physics of Solids in Intense Magnetic Fields* (Plenum, New York, 1969), p. 246.

<sup>16</sup>A. H. Wilson, *Proc. R. Soc. London* **18**, 617 (1928).

<sup>17</sup>L. Wang *et al.* (unpublished); F. M. Mueller (private communication).